

# UW-COSMOS COVID-19 Response

## 1. covid-19 vocabulary indexing/construction

```
"data": [
```

dict\_id": 65,  
name": "covid-19",  
base\_classification": "virus",  
source": "<https://raw.githubusercontent.com/UW-COSMOS/covid-19-vocabulary-indexing/main/vocabularies/covid-19.json>",  
case\_sensitive": true,  
last\_updated": "2020-03-23T05:00:00.000Z",  
term\_hits": {  
 "angiotensin-converting enzyme 2": 3137,  
 "MERS": 40696,  
 "Spike Protein": 95,  
 "N-Protein": 1847,  
 "coronavirus": 76582,  
 "COVID19": 65,  
 "nucleocapsid protein": 13187,  
 "hemagglutinin-esterase": 376,  
 "MERS-CoV": 26365,  
 "SARSr-CoVs": 69,  
 "SARS-CoV": 43257,  
 "TMPRSS2": 10036,  
 "S Protein": 3748,  
 "N Protein": 1847,  
 "S-Protein": 3748,  
 "ACE2": 33836,  
 "betacoronavirus": 773,  
 "COVID-19": 3492,  
 "SARS-CoV-2": 1784,  
 "2019-nCoV": 2704,  
 "SARS": 152805  
}



## 2. targeted document retrieval & aggregation

>33,000 coronavirus-related full-text documents, adding ~2,000 per day

Vocabulary labelled, snippets exposed via API

```
},  
{  
    "pubname": "Journal of Chinese Governance",  
    "publisher": "Taylor and Francis",  
    "_gddid": "5e79e1b7998e17af82660e44",  
    "title": "Experts' conservative judgment and containment of COVID-19 in early outbreak",  
    "doi": "10.1080/23812346.2020.1741240",  
    "coverDate": "",  
    "URL": "https://www.tandfonline.com/doi/full/10.1080/23812346.2020.1741240",  
    "authors": "Qi, Ye; Du, Coco Dijia; Liu, Tianle; Zhao, Xiaofan; Dong, Changgui",  
    "highlight": [  
        "present the case of the outbreak and containment of COVID19 in its early stage and analyze the causes"  
    ]  
},  
{  
    "pubname": "International Journal of Infectious Diseases",  
    "publisher": "Elsevier",  
}
```

generation and release of trained embedding models

## 3. document segmentation

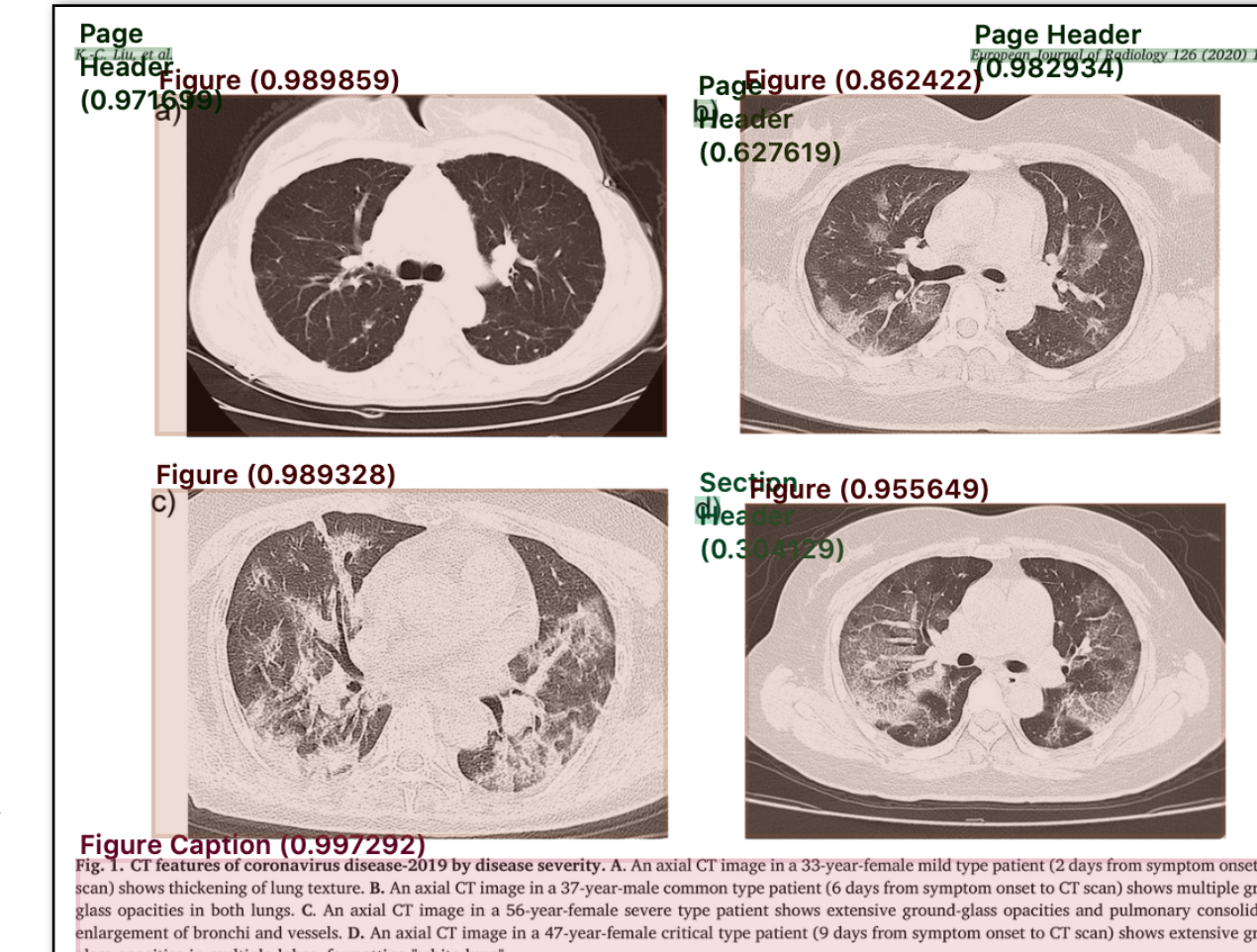


Figure (0.997292)				
Fig. 1. CT features of coronavirus disease-2019 by disease severity. A. An axial CT image in a 33-year-female mild type patient (2 days from symptom onset to CT scan) shows thickening of lung texture. B. An axial CT image in a 37-year-male common type patient (6 days from symptom onset to CT scan) shows multiple ground-glass opacities in both lungs. C. An axial CT image in a 55-year-female severe type patient shows extensive ground-glass opacities and pulmonary consolidation, enlargement of bronchi and vessels. D. An axial CT image in a 47-year-female critical type patient (9 days from symptom onset to CT scan) shows extensive ground-glass opacities in multiple lobes, formatting "white lung".				
Body Text (0.992399)				
3.2.2. CT manifestations of disease improvement				
During follow-up, twelve patients (16 %) dramatically improved. A new CT showed that lesions had decreased in size by more than half in 8 cases (67 %, 8/12) after the patients had received antiviral and supportive treatment after one week of hospital admission. Among them, 3 patients showed remarkable absorption (Fig. 2). Four other patients showed residual interstitial abnormalities with persisting septal lines.				
In the present study, the patients with mild type pneumonia had no obvious changes on CT images. Ground-glass opacities were the most common manifestation, in either the common or severe type patients. Most of the lesions were distributed along the bronchovascular bundle or the dorsolateral and subpleural part of the lungs and were seen with or without interlobular septal thickening. These changes might reflect fluid exudation in the alveolar lumen, secondary to dilation and congestion of alveolar septal capillary, and interstitial edema in the interlobular septa.				
Pulmonary consolidation is mainly found in severe and critical types				
Body Text (0.998753)				
than 5%; the latter is even more time-consuming. CT imaging can demonstrate typical features making the diagnosis of COVID-19 quite likely, which can help to rapidly screen patients, and to stratify the patients' severity to quickly develop effective treatment strategies.				
In the present study, the patients with mild type pneumonia had no obvious changes on CT images. Ground-glass opacities were the most common manifestation, in either the common or severe type patients. Most of the lesions were distributed along the bronchovascular bundle or the dorsolateral and subpleural part of the lungs and were seen with or without interlobular septal thickening. These changes might reflect fluid exudation in the alveolar lumen, secondary to dilation and congestion of alveolar septal capillary, and interstitial edema in the interlobular septa.				
Pulmonary consolidation is mainly found in severe and critical types				
Section Header (0.997304)				
Body Text (0.998753)				
3.2.2. CT manifestations of disease improvement				
During follow-up, twelve patients (16 %) dramatically improved. A new CT showed that lesions had decreased in size by more than half in 8 cases (67 %, 8/12) after the patients had received antiviral and supportive treatment after one week of hospital admission. Among them, 3 patients showed remarkable absorption (Fig. 2). Four other patients showed residual interstitial abnormalities with persisting septal lines.				
In the present study, the patients with mild type pneumonia had no obvious changes on CT images. Ground-glass opacities were the most common manifestation, in either the common or severe type patients. Most of the lesions were distributed along the bronchovascular bundle or the dorsolateral and subpleural part of the lungs and were seen with or without interlobular septal thickening. These changes might reflect fluid exudation in the alveolar lumen, secondary to dilation and congestion of alveolar septal capillary, and interstitial edema in the interlobular septa.				
Pulmonary consolidation is mainly found in severe and critical types				
Table (0.989456)				
Table 2				
The location and morphology of pulmonary lesions in different types in Coronavirus Disease-19 patients [n (%)].				
	mild type (n = 6)	common type (n = 43)	severe type (n = 21)	critical type (n = 3)
Unilateral Lung Involvement	0	15 (35 %)	0	0
Bilateral Lungs Involvement	3 (50 %)	28 (65 %)	21 (100 %)	3 (100 %)
Unique Ground-glass Opacities	0	12 (28 %)	0	3 (100 %)
Multiple Ground-glass Opacities	0	31 (72 %)	16 (76 %)	3 (100 %)
Paving Stone Sign	0	15 (35 %)	10 (48 %)	3 (100 %)
Consolidation	0	0	5 (24 %)	3 (100 %)
Bronchial Wall Thickening	0	2 (5%)	14 (67 %)	3 (100 %)
Pleural Effusion	0	0	0	3 (100 %)
Thickening of Lung Texture	3 (50 %)	40 (93 %)	19 (90 %)	3 (100 %)
No Lung Abnormality	3 (50 %)	0	0	0

COSMOS AI-powered document segmentation over novel corpus

# UW-COSMOS COVID-19 Response

Figure (0.989859)



Figure (0.989328)

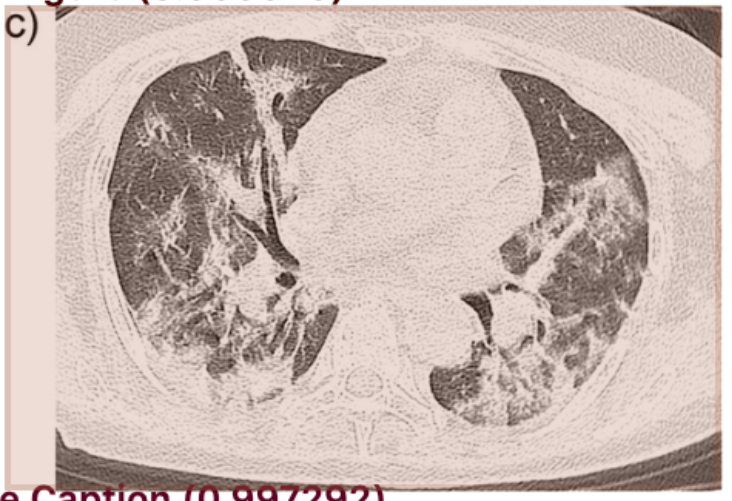


Figure Caption (0.997292)

Fig. 1. CT features of coronavirus disease-2019 by disease severity. A. An axial CT image in a 33-year-female mild type patient (2 days from symptom onset to CT scan) shows thickening of lung texture. B. An axial CT image in a 37-year-male common type patient (6 days from symptom onset to CT scan) shows multiple ground-glass opacities in both lungs. C. An axial CT image in a 56-year-female severe type patient shows extensive ground-glass opacities and pulmonary consolidation, enlargement of bronchi and vessels. D. An axial CT image in a 47-year-female critical type patient (9 days from symptom onset to CT scan) shows extensive ground-glass opacities in multiple lobes, formatting "white lung".

Body Text (0.992399)

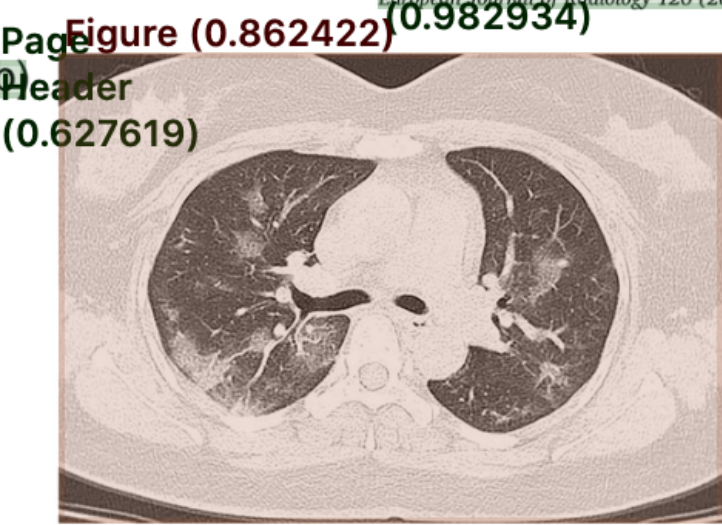
## 3.2.2. CT manifestations of disease improvement

During follow-up, twelve patients (16 %) dramatically improved. A new CT showed that lesions had decreased in size by more than half in 8 cases (67 %, 8/12) after the patients had received antiviral and supportive treatment after one week of hospital admission. Among them, 3 patients showed remarkable absorption (Fig. 2). Four other patients showed residual interstitial abnormalities with persisting septal lines.

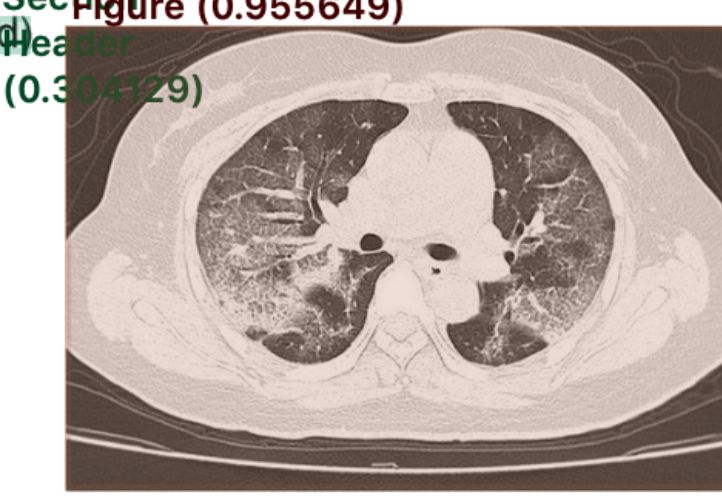
## Section Header Discussion

Body Text (0.997304)

Conventional PCR of sputum, throat swab and lower respiratory tract secretion or sequencing of virus gene represents the gold standard technique for the diagnosis of COVID-19 [8,9]. However, the testing requires at least several hours, and has a false negative rate of more



Section  
Header  
(0.304129)



Body Text (0.998753)

than 5%; the latter is even more time-consuming. CT imaging can demonstrate typical features making the diagnosis of COVID-19 quite likely, which can help to rapidly screen patients, and to stratify the patients' severity to quickly develop effective treatment strategies.

In the present study, the patients with mild type pneumonia had no obvious changes on CT images. Ground-glass opacities were the most common manifestation, in either the common or severe type patients. Most of the lesions were distributed along the bronchovascular bundle or the dorsolateral and subpleural part of the lungs and were seen with or without interlobular septal thickening. These changes might reflect fluid exudation in the alveolar lumen, secondary to dilation and congestion of alveolar septal capillary, and interstitial edema in the interlobular septa.

Pulmonary consolidation is mainly found in severe and critical types

Table (0.989456)

Table 2 The location and morphology of pulmonary lesions in different types in Coronavirus Disease-19 patients [n (%)].

	mild type (n = 6)	common type (n = 43)	severe type (n = 21)	critical type (n = 3)
Unilateral Lung Involvement	0	15 (35 %)	0	0
Bilateral Lungs Involvement	3 (50 %)	28 (65 %)	21 (100 %)	3 (100 %)
Unique Ground-glass Opacities	0	12 (28 %)	0	3 (100 %)
Multiple Ground-glass Opacities	0	31 (72 %)	16 (76 %)	3 (100 %)
Paving Stone Sign	0	15 (35 %)	10 (48 %)	3 (100 %)
Consolidation	0	0	5 (24 %)	3 (100 %)
Bronchial Wall Thickening	0	2 (5%)	14 (67 %)	3 (100 %)
Pleural Effusion	0	0	0	3 (100 %)
Thickening of Lung Texture	3 (50 %)	40 (93 %)	19 (90 %)	3 (100 %)
No Lung Abnormality	3 (50 %)	0	0	0

Table (0.776724)

Table 1 Demographics, baseline characteristics of overall 149 patients.

	General data	Overall (N = 149)
Age		45.11 ± 13.35
Sex		Male/Female(81/68)
Height (cm)		167 (11.75)
Weight (kg)		65.92 (18.75)
BMI		23.75 (4.54)
Exposure history		
Stay in Wuhan		80(53.69%)
stay in Hubei Province except Wuhan		5(3.36%)
Contact with people from Hubei Province		49(32.89%)
No relation with Hubei Province		15(10.06%)
Chronic disease		
cardio-cerebrovascular disease		28(18.79%)
digestive system diseases		8 (5.37%)
endocrine diseases		9(6.04%)
malignant tumor		2(1.34%)
neural system diseases		0(0%)
respiratory system diseases		1(0.67%)
others		4(2.68%)
Temperature (°C)		37.86±0.87
pH		7.11 (0.04)
increased		21 (14.09%)
decreased		4 (2.68%)
PaO <sub>2</sub> (kpa, range80–100)		96.05 (25.58)
decreased		23 (15.44%), 56.25 ± 6.58
SaO <sub>2</sub> (range≥95%)		97.43% (2%)
decreased		14 (9.4%)
Heart rate (beats per minute)		88.63 ± 14.27
Systolic pressure (mmHg)		129.98 ± 15.44
Diastolic pressure (mmHg)		81.69 ± 10.16

BMI: body mass index; PH: hydrogen ion concentration.

Page Header (0.800970)  
BRIEF COMMUNICATION

Body Text (0.808039)  
Three children who recovered from novel coronavirus  
Section Header  
2019 pneumonia

Body Text (0.997827)

In December 2019, a cluster of acute respiratory illness, now known as novel COVID-19, occurred in Wuhan, Hubei Province, China.<sup>1–5</sup> The disease rapidly spread from Wuhan to other areas. Previous studies suggest that COVID-19 is more likely to infect older adult men, particularly those with chronic comorbidities.<sup>6–8</sup> In the isolation ward of the children's hospital affiliated to Zhengzhou University, three children were hospitalised with pneumonia caused by 2019 novel coronavirus (COVID-19). Two were sisters, aged 6 and 8 years old and one was a 6-month-old boy. All three patients had fever, and two had nasal congestion and rhinitis, associated with fatigue, diarrhoea and headache. The 6-year-old girl mainly had cough. None had dyspnoea or cyanosis. Their computerised tomographic scans are shown in Figures 1–3. None of the children required intensive care or mechanical ventilation or had any severe complications.

The time between admission and diagnosis was 2 days. Families of all three children had at least one infected relative, with the children's infection occurring after the parents' infection. The

Figure (0.969785)



Figure Caption (0.986687)

Fig. 3 Computerised tomographic scan of 6-month-old boy.

Body Text (0.997511)

two sisters had family members who visited Wuhan. The other child had no direct link to Wuhan.

Throat swab, sputum, stool and blood samples were tested for COVID-19 nucleic acid using reverse-transcriptase polymerase chain reaction. All three children are confirmed cases. According to the current conditions of the reported cases, the three children mainly belong to family cluster cases.

The children were closely monitored in hospital. The two sisters, but not the infant, were treated with nebulised interferon- $\alpha$  2b 100 000 IU/kg, twice daily for 7 days.

The children's fever resolved within 3 days and after 1 week their symptoms improved significantly. The children were discharged after 10 days, when they had two consecutive negative polymerase chain reaction tests of respiratory specimens at least 1 day apart. However, they required home isolation for 14 days after discharge. The girls were given psychological support by nursing staff. Strict infection control measures were instituted, although the 6-month-old needed special isolation because he was unable to wear a mask.

Very few cases have been reported of children infected with COVID-19.<sup>1–9</sup> The Children's Hospital affiliated to Zhengzhou University is a first-class Children's Hospital in the province. It was designated as one of the regional medical centres by the state in 2019. It is also the designated hospital for medical treatment of children with COVID-19 pneumonia, and is the children's medical centre of Henan Province. At present, the hospital has sent more than medical staff to support Wuhan. The three children were the first children to be managed in Henan Province. Through everybody's effort, careful treatment, psychological nursing support and infection control measures in hospital, these

Figure (0.990268)

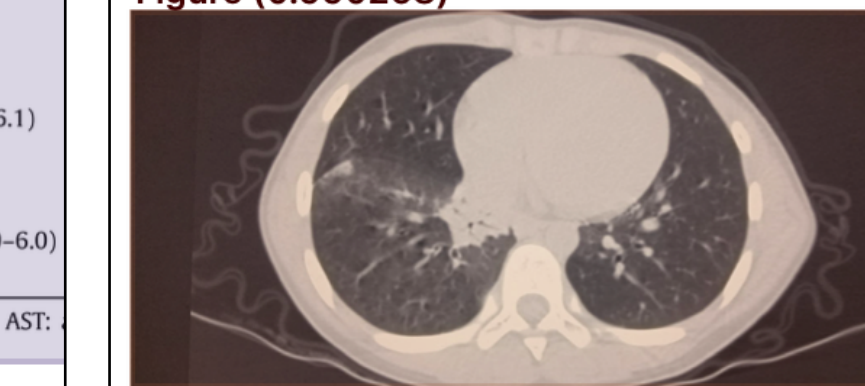


Figure Caption (0.992492)

Fig. 1 Computerised tomographic scan of 8-year-old girl.

Figure (0.981846)



# UW-COSMOS COVID-19 Response

## COSMOS Model results

### 1. Page-level extractions

Regions of interest extracted and classified for further knowledge-base processing.

### 2. Searchable knowledge base

Knowledge base of equations, figures, and tables extracted from page-level information and searchable based on contextual information linked by the model.

### About

The COSMOS Visualizer web application provides an interface to training data, model components, and results for the COSMOS knowledge-base construction pipeline. The [backend](#) (server, database, and API) and [UI components](#) are shared with our Image Tagger training-dataset generation user interface. The user interface components exposed here can be composed and reused for other knowledge-base construction and introspection tasks.

### Credits

This work was funded by DARPA ASKE HR00111990013.

- Visualizer: Daven Quinn, Ian Ross
- Model: Ankur Goswami, Josh McGrath, Paul Luh, and Zifan Liu
- Integration: Ian Ross
- Project lead: Theodoros Rekatsinas, Shanan Peters, and Miron Livny

## Searchable KB pertinent to COVID-19 Literature: searchable over text, tables, figures, equations

Table

Table 4. Output from REML model for square-root transformed average insect and spider biomass, body length and abundance, and diversity collected from a) sweep-netting, and b) pesticide knockdown sampling of emu-wren territories at Portland. Analysis is based on a normal distribution. Asterisks indicate significant results (\*, P < 0.05; \*\*, P < 0.01; \*\*\*, P < 0.001).

	Territory	Season × Habitat type (df 4, 73)		Season (df 1, 73)		Habitat type (df 5, 73)	
		Estimated variance	SE	$\chi^2$	P	$\chi^2$	P
a) Sweep netting samples							
Insect and spider abundance	-0.015	0.089	1.68	0.151	0.88	0.347	1.00 0.418
Insect and spider biomass	0.437	0.683	1.86	0.762	12.24	<0.001***	4.72 0.452
Diversity index (# insect orders+spiders)	0.214	0.262	8.82	0.066	3.91	0.048*	14.64 0.012*
b) Pesticide knockdown samples							
Insect and spider abundance	0.119	0.239	2.36	0.501	5.98	0.014*	6.20 0.184
Insect and spider biomass	0.335	0.859	2.98	0.395	4.25	0.039*	2.81 0.591
Diversity index (# insect orders+spiders)	0.169	0.209	2.94	0.402	9.56	0.002**	7.65 0.105

and Maguire Grainne S., *Territory quality, survival and reproductive success in southern emu-wrens Stipiturus malachurus*, *Journal of Avian Biology*, 37(6), 2006, DOI: 10.1111/j.2006.0908-8857.03757.x

[Preview table](#) [Download pickled pandas dataframe](#) [Download OCRed text](#) [See full stored object](#)

**JSON object for each element**  
preliminary data frame extraction from tables

# **UW-COSMOS COVID-19 Response**

## **datasets/tools to be generated and made available**

- Automated document acquisition and indexing pipeline prioritizing COVID-19 content defined by vocabularies; ~33K relevant documents: *currently active, acquiring ~2k/day*
- Flexible ElasticSearch-powered API endpoint operating over all document full texts; retrieves contextual snippets + reference information: *available publicly now*
- Ability to deploy ASKE/agency team container code over COVID-19 corpus and return derived data products, with full reference information: *available now, (subject to effort availability)*
- Word and document embedding models trained over COVID-19 documents, open interfaces for exploring them: *available publicly within week*
- Open web interface for searching over text, tables, figures, equations in COVID-19 document set: *available publicly within week*
- Database consisting of JSON representations of text, tables, figures, equations for COVID-19 relevant publications: *available to ASKE/agency collaborators within week*